EURASIP Journal on Applied Signal Processing 2005:11, 1656–1667

Performance Evaluation at the System Level of Reconfigurable Space-Time Coding Techniques for HSDPA

Kostas Peppas

Institute of Communication and Computer Systems, National Technical University of Athens, 9 Heroon Polytechniou, 15773 Zografou, Athens, Greece
Email: peppas@telecom.ntua.gr

Angeliki Alexiou

Wireless Research, Bell Labs, Lucent Technologies, The Quadrant, Stonehill Green, Swindon SN5 7DJ, UK
Email: alexiou@lucent.com

Fotis Lazarakis

Institute of Informatics and Telecommunications, National Center for Scientific Research "Demokritos," Ag. Paraskevi, 15310 Athens, Greece
Email: flaz@iit.demokritos.gr

Tareq Al-Gizawi

Institute of Communication and Computer Systems, National Technical University of Athens, 9 Heroon Polytechniou, 15773 Zografou, Athens, Greece
Email: tarek@btsgr.com

Dimitrios I. Axiotis

Institute of Communication and Computer Systems, National Technical University of Athens, 9 Heroon Polytechniou, 15773 Zografou, Athens, Greece
Email: jaxiot@telecom.ntua.gr

Received 15 March 2004; Revised 15 December 2004

A reconfigurable space-time coding technique is investigated, for a high-speed downlink packet access multiple-antenna network, which combats the effects of antenna correlation. Reconfigurability is achieved at the link level by introducing a linear precoder in a space-time block coded system. The technique assumes knowledge of the long-term characteristics of the channel, namely the channel correlation matrix at the transmitter. The benefits of the proposed reconfigurable technique as compared to the conventional non-reconfigurable versions are evaluated via system-level simulations. In order to characterize the system-level performance accurately and, at the same time, use a feasible approach in terms of computational complexity, a suitable link-to-system interface has been developed. The average system throughput and the number of satisfied users are the performance metrics of interest. Simulation results demonstrate the performance enhancements achieved by the application of reconfigurable techniques as compared to their conventional counterparts.

Keywords and phrases: space-time block coding, linear precoding, reconfigurability, system-level performance, link-to-system level interface, high-speed downlink packet access.

1. INTRODUCTION

Future-generation wireless systems design is expected to address a number of challenges, such as high data rates, improved link quality, and *reconfigurability*, that is, adaptivity to varying propagation and network conditions. These requirements set a strong demand for significant advances in both radio access and network technology, highlighting the importance of *reconfigurable transceiver architectures both horizontally (adaptive transceiver architectures within the context of one wireless access technology) and vertically (adaptive transceiver architectures to support one of multiple wireless*

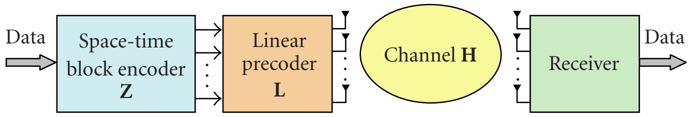

Figure 1: Reconfigurable transmission scheme combining space-time block codes and a linear transformation designed to exploit the channel knowledge available at the transmitter.

access technologies). In order to address reconfigurability, promising technologies, such as space-time processing, can be considered as a baseline and new features that provide adaptivity to varying propagation or network conditions need to be designed. An example of such a reconfigurable transceiver architecture will be presented in the following section.

The requirements, in terms of computational and hardware complexity, and performance enhancements resulting from incorporating multiple-input multiple-output (MIMO) techniques in a wireless network need to be evaluated in a realistic manner, in order to assess their efficiency. The importance of system-level evaluation of space-time processing techniques is critical, as the performance gains obtained by the application of these techniques at the link level may not translate to equivalent gains at the system level. On the other hand, the evaluation of the benefits of MIMO techniques at the system level introduces a number of challenges, such as the requirement for suitable spatio-temporal channel modeling and optimization of the trade-off between simulation complexity and accuracy, by means of the identification of a suitable link to system-level interface. The system-level simulator input should be specified according to a predefined number of test cases, each consisting of specific space-time algorithms, antenna configurations, propagation environment, mobility, and user requirements.

In this paper, the system-level performance of high-speed downlink packet access (HSDPA) networks enhanced by means of reconfigurable space-time coding techniques is investigated. The work presented herein was partly performed within the framework of the IST-FITNESS project (http://www.telecom.ece.ntua.gr/fitness).

The main objectives of this study are (i) to evaluate the impact of the variation of critical link-level parameters, such as the antenna correlation, on the performance of a multiple-antenna HSDPA network, and (ii) to assess the performance enhancements at the system level achieved by the application of reconfigurable space-time coding techniques.

The paper is organized as follows. The reconfigurable space-time coding technique performed at the link level is presented in Section 2. The link to system-level interface is presented in Section 3 and the basic system simulation assumptions, in terms of network deployment, propagation issues, and user services, are explained in Section 4. In Section 5, the system-level simulation methodology is described. In Section 6, simulation results and validation of the benefits of reconfigurable space-time techniques as compared to their conventional counterparts are illustrated. Finally, the paper is concluded in Section 7.

2. LINK-LEVEL RECONFIGURABILITY WITH LINEAR PRECODING

The impact of antenna correlation on adaptive array techniques has been investigated in [1]. It has been shown that fading correlations reduce MIMO channel capacity and link-level performance in terms of symbol error rate [2, 3]. Nevertheless, considerable capacity and link-level performance gains can be obtained by transmission along the eigenmodes of the transmit antenna correlation matrix [4]. In [5], an optimal linear precoder is proposed that assumes knowledge of the transmit antenna correlations and improves the performance of a space-time coded system. Assuming a flat fading channel and a maximum-likelihood receiver, the optimal precoder forces transmission only on the nonzero eigenmodes of the transmit antenna correlation matrix. This is referred to as *eigenbeamforming*. The power allocation policy on the eigenmodes is given by a *water-pouring* solution. The main advantage of the above linear precoder is that it does not have to track fast fading, but only the structure of slowly varying antenna correlations. The latter can be fed back to the transmitter using a low-rate feedback link.

The impact of antenna correlation on the link-level performance of orthogonal [6, 7] and quasiorthogonal [8] space-time block coded systems has been investigated in [9], where linear precoders, which achieve reconfigurability to antenna correlation, have been formulated for space-time block coded systems with any number of transmit and receive antennas.

In the analysis presented in this paper, a two-transmit-, two-receive-antenna system is assumed, which employs Alamouti space-time block coding [6]. The space-time block encoder, denoted by $\mathbf{Z}$, maps the input data sequence $\mathbf{x} = (x_1, x_2)$ to be transmitted into a 2×2 matrix $\mathbf{Z} = \begin{bmatrix} x_1 & x_2 \\ -x_2^* & x_1^* \end{bmatrix}$ of codewords that are split on a set of two parallel sequences.

Reconfigurability is introduced by applying linear precoding to the space-time block encoder (as depicted in Figure 1), denoted by the linear transformation matrix $\mathbf{L}$ and determined so as to minimize a given criterion, such as an upper bound on the pairwise error probability (PEP) of a codeword.

The received signal $\mathbf{Y}$, corrupted by additive white Gaussian noise denoted by the 2×2 matrix $\mathbf{\Sigma}$ with covariance matrix $\sigma^2\mathbf{I}_2$, where $\mathbf{I}_2$ is the 2×2 identity matrix, is given by

$$\mathbf{Y} = \mathbf{HLZ} + \mathbf{\Sigma}. \quad (1)$$

Each entry h_{ji} of the 2×2 channel matrix $\mathbf{H}$ represents the channel response between transmit antenna i and receive antenna j.

The received signal (at the mobile) is assumed to be a linear combination of several paths reflected from local scatterers, which results in uncorrelated fading across the receive antennas and therefore uncorrelated rows of the matrix **H**. However, limited scattering at the base station (BS) can cause antenna correlation and therefore correlated columns of **H**. In the general case, a geometry-based stochastic channel model can be used [10], in which the probability density function (PDF) of the geometrical location of the scatterers is prescribed, corresponding to a power Azimuth spectrum (PAS) following a certain distribution. The correlation between two antennas in this case can be calculated from the cross-correlation between the antenna array response elements with respect to the assumed PAS:

$$\rho = R_{XX}(D) + jR_{XY}(D), \tag{2}$$

where $D = 2\pi d/\lambda$, d is the distance between the two antennas, λ is the wavelength, and R_{XX} and R_{XY} are the cross-correlation functions between the real parts (equal to the cross-correlation function between the imaginary parts) and between the real and the imaginary part, respectively:

$$\begin{aligned} R_{XX}(D) &= \int_{-\pi}^{\pi} \cos(D\sin\phi)\,\text{PAS}(\phi)d\phi, \\ R_{XY}(D) &= \int_{-\pi}^{\pi} \sin(D\sin\phi)\,\text{PAS}(\phi)d\phi, \end{aligned} \tag{3}$$

with φ the azimuth angle parameter.

In the analysis performed in this paper, in order to characterize performance *as a function* of the antenna correlation, a correlation-based model [10] was selected instead. According to this model, the channel **H** can be written as follows:

$$\mathbf{H} = \mathbf{H}_W \mathbf{R}_T^{1/2}, \tag{4}$$

where $\mathbf{H}_W$ is a 2×2 i.i.d. complex matrix and $\mathbf{R}_T$ is the 2×2 transmit antenna correlation matrix.

For the general case of a system with M transmit and N receive antennas employing space-time block coding, it is shown in [9] that the linear precoder **L** can be designed to minimize an upper bound on the average *pairwise error probability*. The PEP is defined as the error probability of choosing a certain codeword $\mathbf{Z}^l$ instead of the actually transmitted codeword $\mathbf{Z}^k$. An upper bound on the average PEP is [9]

$$\overline{\text{PEP}} \le \left[\det(\mathbf{I} + \mathbf{D})\right]^{-N}, \tag{5}$$

where N is the number of receive antennas and $\mathbf{D} = (E_s/\sigma^2)\mathbf{R}_T^{1/2}\mathbf{L}\mathbf{E}\mathbf{E}^H\mathbf{L}^H\mathbf{R}_T^{1/2^H}$, with E_s the symbol energy, σ^2 the noise variance, and **E** the *minimum-distance code error matrix*. If $\widetilde{\mathbf{E}}(k,l,t) = \mathbf{Z}^k(t) - \mathbf{Z}^l(t)$ is the code error matrix, the minimum-distance code error matrix is defined as

$$\mathbf{E} = \arg\min_{\widetilde{\mathbf{E}}(k,l,t)} \det\left[\widetilde{\mathbf{E}}(k,l,t)\widetilde{\mathbf{E}}^H(k,l,t)\right]. \tag{6}$$

The design of the linear precoder also satisfies a certain power constraint condition:

$$\text{Trace}\left(\mathbf{L}\mathbf{L}^H\right) = P_0. \tag{7}$$

The linear precoder is computed by solving the minimization of the average PEP under the power constraint given in (7):

$$\begin{aligned} \mathbf{L} &= \mathbf{V_r}\mathbf{\Phi_f}\mathbf{V_e}^H, \\ \mathbf{\Phi_f^2} &= \left(\gamma I - \left(\frac{E_s}{\sigma^2}\right)^{-1} \mathbf{\Lambda_r^{-2}\Lambda_e^{-1}}\right)_+, \end{aligned} \tag{8}$$

where the singular value decomposition (SVD) of $\mathbf{R}_T^{1/2}$ and $\mathbf{E}\mathbf{E}^H$ are $\mathbf{R}_T^{1/2} = \mathbf{U_r\Lambda_r V_r}^H$ and $\mathbf{E}\mathbf{E}^H = \mathbf{U_e\Lambda_e V_e}^H$, respectively, $\gamma > 0$ is a constant computed from the power constraint and $(\cdot)_+$ stands for max $(\cdot, 0)$.

For orthogonal space-time block coded systems, $\mathbf{E}\mathbf{E}^H$ is a scaled identity matrix ($\mathbf{V_e} = \mathbf{I}$) and the precoder is independent of the matrix **E**.

In the specific case of a two-transmit-, two-receive-antenna system that employs Alamouti space-time block coding [6] and assuming $\lambda_{r,1}$, $\lambda_{r,2}$ are the eigenvalues and $[w_1, w_2]^T$ the strongest eigenvector of the correlation matrix $\mathbf{R}_T^{1/2}$, the following three cases are identified for the precoder.

(i) When the antenna correlation is less than 1, $\lambda_{r,1}, \lambda_{r,2} \neq 0$. In this case, for $\beta = (1/\lambda_{r,2}^2 - 1/\lambda_{r,1}^2)/(E_s/\sigma^2) \le 1$, the precoder can be written as

$$\mathbf{L} = \frac{1}{\sqrt{2}}\begin{bmatrix} w_1 & w_2^* \\ w_2 & -w_1^* \end{bmatrix}\begin{bmatrix} \sqrt{1+\beta} & 0 \\ 0 & \sqrt{1-\beta} \end{bmatrix}. \tag{9}$$

(ii) When the antenna correlation is zero, the eigenvalues of the matrix $\mathbf{R}_T^{1/2}$ are equal and therefore $\beta = 0$. In this case, the precoder **L** becomes

$$\mathbf{L} = \frac{1}{\sqrt{2}}\begin{bmatrix} w_1 & w_2^* \\ w_2 & -w_1^* \end{bmatrix} \tag{10}$$

and the transmission scheme is equivalent to orthogonal space-time block coding (Alamouti).

(iii) When the antenna correlation is 1, only one eigenvalue of the matrix $\mathbf{R}_T^{1/2}$ is nonzero. In this case, $\beta = 1$, $\mathbf{\Phi_f^2} = \begin{bmatrix} 1 & 0 \\ 0 & 0 \end{bmatrix}$ and the precoder **L** becomes

$$\mathbf{L} = \begin{bmatrix} w_1 & 0 \\ w_2 & 0 \end{bmatrix}. \tag{11}$$

The transmission scheme is equivalent to a beamformer.

An example system architecture for the incorporation of the linear precoder, which supports reconfigurability to antenna correlation, is depicted in Figure 2, where the conventional HSDPA transceiver scheme has been modified to accommodate the reconfigurability feature. The new modules are **L**, **COR**, and **STD**.

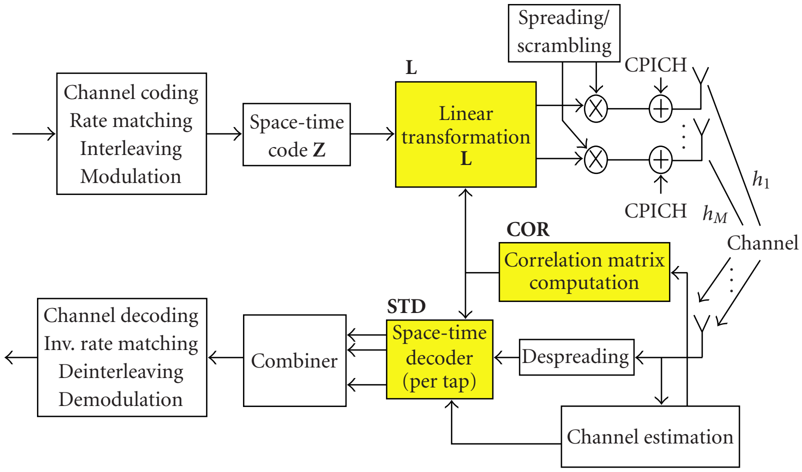

FIGURE 2: Reconfigurability to antenna correlation—transceiver architecture for HSDPA.

At the transmitter, the linear precoder (**L**) is applied to the space-time encoded symbols. A generalized space-time block encoder **LZ** is needed to replace the conventional space-time encoder **Z**. In order to compute the linear precoder coefficients, the correlation matrix is computed (**COR**) based on channel information fed back from the receiver. In an HSDPA environment, for example, this information may be available from the feedback bits sent by the mobile station.

At the receiver, the generalized space-time block decoder (**STD**) has a structure identical to the conventional space-time block decoder, but needs to consider, instead of the channel estimates, the equivalent channel **HL**, defined as the linear transformation of the channel according to the coefficients of **L**. The correlation computation module also resides at the receiver side, where, based on the channel estimates, the correlation coefficients are stored and used for the generalized space-time block decoding. In the case of multiple receive antennas, maximal ratio combining is applied.

In the analysis carried out in this paper, the antenna correlation is assumed perfectly known at the transmitter. Further investigation of the sensitivity [11] of the precoder to inaccurate channel state information used for the computation of the antenna correlation has demonstrated *robustness* to channel estimation errors.

As shown in [9], the performance of the Alamouti space-time block coding scheme degrades when the antenna correlation increases, whereas high antenna correlation is beneficial for the beamforming performance. The proposed scheme performs similarly to space-time block coding for low antenna correlation values and becomes equivalent to beamforming for high antenna correlation values. For correlation values between the two extremes, the proposed approach outperforms both conventional schemes. In Figure 3, an example is given of the performance of a 2 × 2 HSDPA transceiver, in terms of required transmit bit signal-to-noise ratio (E_b/N_0) for 1% frame error rate (FER). The proposed reconfigurable approach is compared to the conventional Alamouti, denoted by STTD and described by (10), and beamforming denoted by BF and described by (11). The link-level simulation assumptions are listed in Table 1.

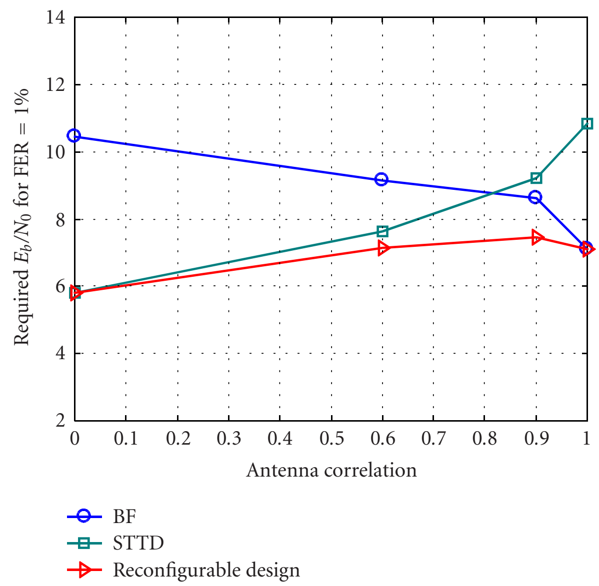

FIGURE 3: Reconfigurability to antenna correlation for two transmit and two receive antennas at 5.4 Mbps.

3. LINK-TO-SYSTEM INTERFACE

Performance gains achieved on a single communication link (*link level*) do not necessarily translate into equivalent gains at the *system level*, where multiple base stations communicate with multiple users. In order to perform a realistic evaluation of the performance enhancements achieved by advanced multiple-antenna and coding schemes, system-level simulations need to be considered. In addition to modeling intracell interference, such system-level simulations would also model the interaction between multiple cells in the form of intercell interference.

TABLE 1: HSDPA link-level simulation assumptions.

Parameter	Value
Spreading factor	16
Number of codes	15
Modulation	QPSK, 16-QAM
Code rate	1/4, 1/2, 3/4
Data rates	1.8, 3.6, 5.4, 10.8 Mbps
CPICH power	10%
TTI length	2 ms
MIMO channel model	Flat, correlation-based
UE speed	0 km/h
Channel estimation	Ideal
Antenna configuration	2Tx, 2Rx

One of the major difficulties in realizing a system-level simulation is the complexity involved in identifying the performance of the radio links between all terminals and base stations. Link-level simulation of such a large number of links is clearly prohibitive. As a result, the performance of the radio link has traditionally been evaluated in terms of FER as a function of signal-to-interference-plus-noise ratio (SINR), averaged over all channel realizations. FER versus SINR performance curves have therefore been used as the interface between the link- and system-level simulators (*average value interface*). This may be adequate for circuit-switched voice-centric radio networks where a large number of different radio channel realizations may be observed over the duration of a coding block. With data-centric radio networks, however, the relatively short packet durations—as compared to the channel coherence time—imply that only a single channel realization is typically encountered over the duration of a coding block. A specific channel realization encountered may result in performance, that is significantly different from the one predicted from the average FER versus SINR curves, which could have a significant impact on crucial system-level mechanisms such as packet scheduling.

A suitable interface between link- and system-level simulations for a packet radio system should be described by a metric, which can appropriately encapsulate the performance of the receiver, say in terms of the probability of frame error, given the prevailing radio environment (specific channel realization) over the packet duration. The goal is to be able to evaluate the probability of frame error at any instant for a particular user, given the user's $N \times M$ channel matrix $\mathbf{H}$ (M transmit and N receive antennas are assumed in the general case), interfering channel matrices $\mathbf{H}_1, \mathbf{H}_2, \dots, \mathbf{H}_K$, symbol energy E_s, and thermal noise energy N_0 (*actual value interface*). This can be envisaged in terms of curves of the form

$$\text{FER} = f\left(C_I\left(\mathbf{H}, \mathbf{H}_1, \dots, \mathbf{H}_K, E_s, N_0\right)\right), \tag{12}$$

where $C_I = C_I(\mathbf{H}, \mathbf{H}_1, \dots, \mathbf{H}_K, E_s, N_0)$ is a scalar performance metric. As the mapping between a large number of parameters $(\mathbf{H}, \mathbf{H}_1, \dots, \mathbf{H}_K, E_s, N_0)$ to FER performance is not feasible, the basic idea in identifying an interface metric like C_I is to select a suitable *compression* function between this large number of resource elements to a smaller number (scalar in this case) before mapping to FER performance. The identification of a suitable scalar metric, which is a function of all channel, interference, and noise parameters and can provide an adequate (one-to-one) *mapping* to FER performance, is a challenging task.

We consider a radio packet being received, passing through an $N \times M$ channel matrix $\mathbf{H}$, in the presence of only additive white Gaussian noise of energy N_0. Then,

$$\text{FER} = f\left(C_I\left(\mathbf{H}, E_s, N_0\right)\right). \tag{13}$$

The use of the information-theoretic channel capacity C [12] has been proposed [13] as a suitable interface metric C_I, in this case

$$C_I = C = \log_2 \det\left(\mathbf{I}_N + \frac{1}{M}\frac{E_s}{N_0}\mathbf{H}\mathbf{H}^H\right), \tag{14}$$

where $\mathbf{I}_N$ is the identity matrix. It can be shown that this interface is also suitable for a space-time block coded system with multiple receive antennas [14]. Furthermore, the capacity metric under the assumption of Gaussian interference, where only the received power of the interfering users is accounted for and not their channel structure, was shown [14] to be a suitable link to system-level interface metric in the case of a large (> 2) number of intercell interferers. Based on this observation and the relatively low computational complexity, this metric was selected for the link-to-system interface employed in the analysis carried out in this paper.

The evaluation of a link-to-system interface "lookup" curve consists of the computation of a large number of (FER, C_I) pairs satisfying (13). In other words, for a fixed value of $(\mathbf{H}, E_s, N_0)$, link-level simulations are carried out and the average FER is evaluated. The value of the metric C is computed according to (14). The same experiment is repeated for a large number of values of $(\mathbf{H}, E_s, N_0)$, aiming at spanning the whole range of interest of FER. Ideally, for the mapping to be one-to-one, the set of (FER, C) points must lie on a linear curve. In practice, deviation from the one-to-one mapping is when employing more than one receive antenna. This deviation is due to the fact that, although in the single-receive-antenna case, the capacity metric is uniquely characterized by a single eigenvalue of the channel, in the multiple-receive-antenna case, multiple eigenvalues determine the capacity metric value. In the study performed herein, up to two eigenvalues determine the capacity metric depending on the channel rank. Small perturbations on the eigenvalues may result in the same instantaneous capacity but slightly different FER. As shown in [14], such deviations are negligible. Interpolation can be employed in this case in order to derive a single interface curve suitable for the implementation of the mapping.

As explained in the previous section, in order to achieve reconfigurability to antenna correlation, the linear precoder $\mathbf{L}$ directs the transmission towards the eigendirections of the correlation matrix $\mathbf{R}_T$ following a water-filling policy.

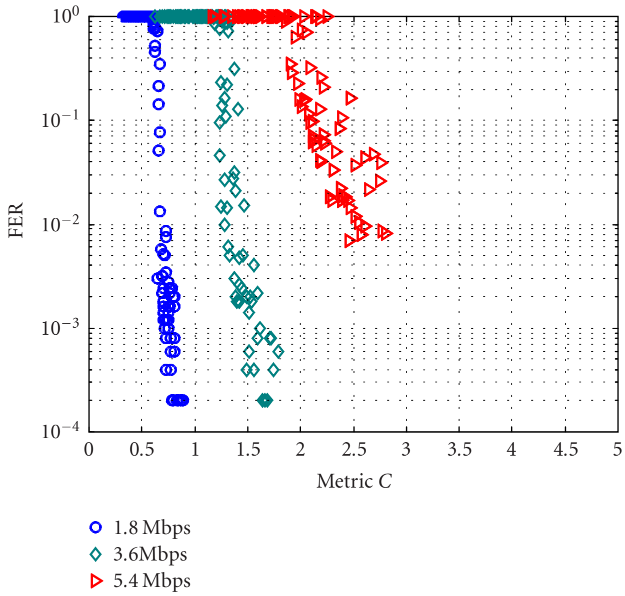

FIGURE 4: Link-to-system interface (antenna correlation = 0.6, 2×2 STTD).

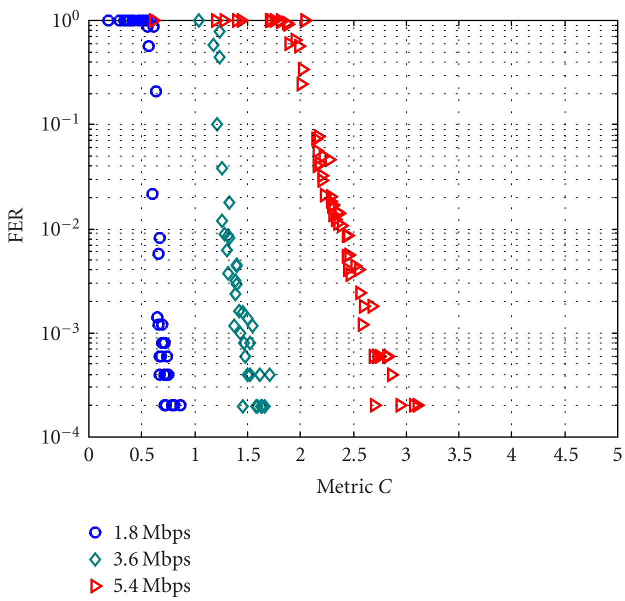

FIGURE 5: Link-to-system interface (antenna correlation = 0.6, 2×2 reconfigurable design).

A suitable link-to-system interface for the reconfigurable case needs to consider instead of the channel estimates, the equivalent channel **HL**, defined as the linear transformation of the channel according to the coefficients of **L**, and is given by the following equation:

$$C = \log_2 \det \left(\mathbf{I}_N + \frac{1}{M} \frac{E_s}{N_0} \mathbf{H}\mathbf{L}\mathbf{L}^H \mathbf{H}^H \right), \qquad (15)$$

where **L** is the precoder matrix.

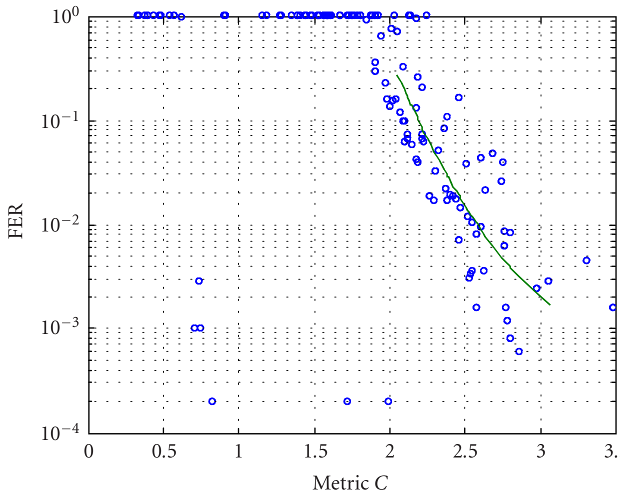

FIGURE 6: Second-degree curve fitting for link-to-system interface (2 × 2 STTD, antenna correlation = 0.6, 5.4 Mbps).

Based on the simulation assumptions illustrated in Table 1, link-to-system interface curves have been evaluated for a number of antenna correlation parameters and data rates for both the Alamouti space-time block coding and the proposed reconfigurable design. The results for antenna correlation equal to 0.6 are depicted in Figures 4 and 5.

In order to derive a single interface curve, interpolation is applied. An example is depicted in Figure 6 for the case of Alamouti space-time block coding with 5.4 Mbps. The corresponding optimum polynomial curve fitting is of the form $f(C) = aC^2 + bC + c$ and the corresponding FER is given by $10^{f(C)}$. In this case, the application of the least-squares method yields the following values for the coefficients of the polynomial $f(C) : a = 1.1025, b = -7.8207, c = 10.853$.

The implementation of the interface between link and system levels consists in the evaluation of the metric C that describes the link of interest at a certain (instantaneous) system-level realization. The instantaneous value of C is computed (see (14) and (15)) as a function of the instantaneous channel matrix **H**, the precoding matrix **L**, and the average received SINR. The average SINR is evaluated taking into account the transmit power, the path loss, and shadow fading for the desirable signal and interfering links from all other cells in the network along with the thermal noise power. For a certain instantaneous value of C, the interface "lookup" curve is used to identify the FER that corresponds to this value.

4. SYSTEM-LEVEL ASSUMPTIONS

The basic assumptions for the implementation of the HSDPA system-level simulator [15] are as follows.

Cell deployment. The HSDPA deployment consists of 19 three-sector sites, as depicted in Figure 7. The sectored architecture is selected for interference reduction and harmonization with the standards [16].

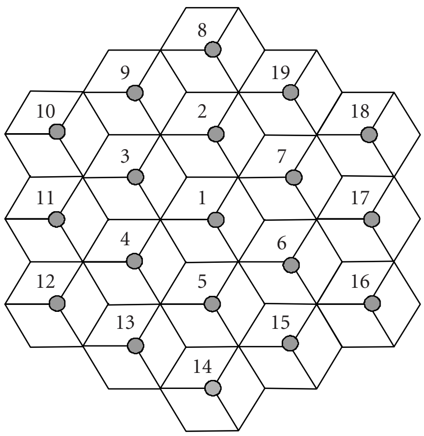

Figure 7: HSDPA cell deployment.

Propagation modeling. Suitable propagation models should be adopted according to the specified deployment scenarios. In an urban and suburban environment, the propagation model introduced in [15] will be used for the HSDPA deployment as shown in the following equation:

$$\mathrm{PL} = 128.1 + 37.6 \log_{10}(R), \tag{16}$$

where PL is the path loss in dB and R is the distance in km. Slow fading is added with standard deviation of 10 dB.

MIMO channel modeling. The MIMO channel model incorporated in the reconfigurable HSDPA simulator is the correlation-based stochastic channel model described in (4). A flat (single-tap) channel model is assumed for the sake of simplicity, as the focus of the analysis is on the impact of antenna correlation. Nevertheless, frequency selectivity can be reflected to a correlation-based model or in a geometry-based stochastic model as analyzed in [10]. Moreover, the approach of the link-to-system interface and system-level methodology is equally applicable to the frequency selective case by considering the channel capacity metric in this case [17].

User mobility. A walking speed mobility scheme is adopted. At the beginning of a simulation run, a user is assigned an initial position, a moving direction, and a speed with values uniformly distributed in [0, 3] km/h.

Services. Two packet-switched services are simulated in the downlink only:

(i) Web browsing with average transmission rate 64 kbps;
(ii) FTP with average transmission rate 384 kbps.

The above rates correspond to the prescribed service rate for Web browsing and FTP. For each service, the service activity factor (SAF) is defined as the percentage of the communication traffic generated by the network subscribers requesting the specific service. In the study carried out in this paper, the SAF is set to 0.6 for the Web users and 0.4 for the FTP users. This means that 60% of the communication traffic within the network is generated by Web users and 40% of the traffic is generated by FTP users.

Traffic pattern. The proposed ETSI data-traffic model in [18] assuming that all users are in an active session is considered. The adoption of this model results in generating a certain load with a smaller number of users, and hence reducing the complexity and simulation time. At the beginning of a simulation trial, the equivalent number of users that generates the given traffic load per sector is uniformly dropped within the network of cells. For the simulation scenarios considered in this paper, the traffic load per sector is 9 Mbps.

We consider the general case where the load per sector is l and the network deployment consists of n cells. The equivalent number of users that generates this traffic load is given by the following equation:

$$\text{No. of users} = \left[\frac{n \cdot l \cdot \mathrm{SAF}}{\text{service\_rate}} \right] + 1, \tag{17}$$

where the symbol $[x]$ denotes the integer part of the real number x. A numerical example of the application of (17) is as follows: for a network deployment that consists of 19 three-sectored sites, $n = 3 * 19 = 57$ sectors. The values for *service_rate* are 64 kbps and 384 kbps for Web browsing and FTP, respectively, whereas $l = 9$ Mbps/sector. The *SAF* is 0.6 and 0.4 for Web browsing and FTP users, respectively. Substituting the corresponding values in (17), the number of users in the network is 4818 for Web browsing and 528 for FTP. It is worth observing that although the percentage of FTP users related to the overall number of the network users is less than 10%, they generate 40% of the communication traffic within the network.

Packet scheduler. Packet scheduling is performed by every sector base station. The users are rank ordered according to their instantaneous capacity C metric. Every user has one source queue where data are generated according to the user service rate. Only one user can be served at every MAC frame. The scheduling is performed on a frame-by-frame basis and the user with the highest C metric is served first. The scheduler continues to transfer data to the user until the entire user's data have been transferred. Once this happens, the user (from the remaining set of users) with the highest instantaneous C metric is served by the base station and the whole process continues until the MAC frame downlink time resources are exhausted.

Performance metrics. The system-level performance is evaluated in terms of user and system throughput as well as the number and percentage of satisfied users.

The throughput is defined as the number of successfully transmitted bits in a specific period of time and is measured in Mbps.

For every user of the network, the *User Throughput* during one frame is computed by the following equation [18]:

$$\text{User Throughput} = \rho_{\text{Mode\_User}} \times (1 - \mathrm{FER}_{\text{user}}), \tag{18}$$

where $\rho_{\text{Mode\_User}}$ is the nominal bit rate of the specific user, which depends on the link quality and $\mathrm{FER}_{\text{user}}$ is the frame error rate for the user obtained through the link-to-system interface described in the previous section. Then, the sector

Table 2: System-level simulation parameters.

Parameter	Value	Comment
Number of cells	19	3 sectors
Cell shape	Hexagonal	—
Cell radius	1400 m	—
Propagation model	PL= $128.1 + 37.6\log_{10}(R)$	R in km
Log normal shadowing	10 dB	—
User mobility	Uniformly distributed in [0, 3 km/h]	Walking speed
MIMO channel	Flat, correlation-based stochastic model	—
Carrier frequency	2000 MHz	—
Overhead channel downlink power usage	20%	CPICH, P-CCPCH, S-CCPCH, SCH, etc.
Base station power	44 dBm	—
Noise power	−99 dBm	—

throughput is calculated by summing the User Throughput for every user within the sector. The System Throughput is obtained by averaging the sector throughput for all the sectors of the network. Finally, the Average *System Throughput* represents the System Throughput averaged over the whole simulation time.

A user is classified as *satisfied* if his/her average throughput, over the session duration, is at least 95% of the corresponding service rate. The number and the corresponding percentage of satisfied users are calculated separately for each service. The overall number/percentage of satisfied users represents the satisfied system users.

Depending on the system load, channel quality, and so forth, a user's average throughput may be smaller than the corresponding service rate. Hence, a performance metric of interest is the average user throughput expressed as a percentage of the service rate.

In Table 2, the system simulation parameters are summarized.

5. SYSTEM-LEVEL SIMULATION METHODOLOGY

In this section, the system simulation methodology is presented. The first step of the system simulation involves the placement of base stations in the coverage area of the wireless network, the placement of the mobiles within each cell, the evaluation of path loss and shadowing from each base station to each mobile, and the identification of a serving base station for each mobile based on the computed losses.

In the main simulation loop, it is checked whether the position of every user should be updated. In this case, the signal strengths between all considered transmitters and receivers are calculated. The average signal-to-interference-plus-noise ratio (SINR) is evaluated taking into account the transmit power, the path loss, and shadow fading for the desirable signal and interfering links from all other cells in the network along with the thermal noise. Link adaptation mechanisms are activated.

For every frame, MIMO channels for the wanted signals at all mobiles need to be simulated. The computation of the MIMO channel matrices takes place in accordance with the channel model proposed in Section 2 and includes fast fading. This procedure is in line with dynamic system-level simulations [19, 20, 21] and is in contrast to traditional system simulation methodology where fast fading is only considered for generating performance curves at the link level. To determine the FER performance of a mobile receiver in conjunction with a specific MIMO channel realization, we make use of the information-theoretic capacity metric C described in (14) and (15) for the non-reconfigurable and reconfigurable cases, respectively.

The performance of the mobile receivers is assessed by consulting precomputed curves ($\text{FER} = f(C)$) like the ones illustrated in Figures 4 and 5, derived from link-level simulations based on different values of the channel matrix $\mathbf{H}$ and SINR. As small deviations from a one-to-one mapping may be observed, and in order to derive a single interface curve, interpolation needs to be applied, as depicted in Figure 6.

At the end of the simulation time, statistical results from the simulated network are gathered and processed. Based on the above description, an outline of the simulation procedure is described in Algorithm 1 in a pseudocode format, where time steps correspond to frame duration. The simulation procedure is also depicted in Figure 8 in flow chart format.

6. SIMULATION RESULTS

The system-level performance is investigated for the reconfigurable and non-reconfigurable space-time block coding HSDPA cases. The single-antenna-test case is also investigated as a reference point, in order to demonstrate the benefits of employing space-time techniques. The system is simulated for 180 seconds. The performance metrics of interest are the user and system throughput and the number and percentage of satisfied users. The equivalent load per sector is considered equal to 9 Mbps and the traffic pattern described in Section 4 is used for different values of the antenna correlation. In Table 3, the system-level performance simulation results are summarized. The first column describes the corresponding test case with the following notation: SISO, NRC, and RC stand for single-input single-output,

Initialization phase
(i) Place a number of mobiles within the geographic area of the network, in accordance with an assumed traffic pattern.
(ii) Evaluate the path loss and shadowing from each base station to each mobile, and allocate a serving base station to each mobile in the system.
For $n = 1$ to N time steps
(i) Update the offered traffic at the base stations for each mobile in accordance with the applied traffic model. Use path and shadow loss, in conjunction with the base station transmit powers, to determine the long-term averaged power levels of the received wanted and interfering signals, and hence the average SINR, at each mobile. Operations such as link adaptation and handover are based on these power levels.
(ii) Compute the channel matrix for the wanted signal in accordance with the channel model described in Section 2. In the case of the reconfigurable design, compute the precoder matrix $\mathbf{L}$ based on the channel matrix for the wanted signal. Evaluate the C metric using (14) or (15), depending on the simulation scenario.
(iii) Determine the performance of each mobile receiver by consulting precomputed curves of the form FER $= f(C)$.
End
End of simulation.

Algorithm 1: System-level simulation procedure.

non-reconfigurable, and reconfigurable, respectively. The following column describes the value of the antenna correlation (0, 0.6, and 0.9). The total number of users in the system, the number of satisfied users, the average system throughput, and the percentage of satisfied users are depicted. It can be observed from Table 3 that a network of SISO base stations cannot efficiently serve a traffic load of 9 Mbps, and similar heavy loads result in a low throughput and a low percentage of satisfied users (5.05 Mbps and 45%, respectively). Thus, for such a heavy load, the incorporation of multiple antennas and the application of space-time processing should be considered, where the conventional 2×2 Alamouti space-time block coding scheme achieves 7.55 Mbps average system throughput and percentage of satisfied users equal to 80.5% for the ideal case of zero antenna correlation (for which the Alamouti approach achieves best performance, as depicted in Figure 3).

An increase in antenna correlation from 0 to 0.9 results in an average throughput decrease from 7.55 Mbps to 6.89 Mbps. The percentage of satisfied Web users decreases from 80.9% to 73.5%, whereas the percentage of satisfied FTP users decreases from 79.1% to 64.3%.

The application of the reconfigurable algorithm, when the antenna correlation is equal to 0.6, achieves a 2.7% improvement in system throughput. The number of satisfied Web users is improved by 3.4% and the number of satisfied FTP users is improved by 5.4%. Finally, the number of overall satisfied system users is improved by 3.6%. It should be noted that the improvement of the number of satisfied system users is very close to the improvement of the number of satisfied Web users since the latter represent around 90% of the total network users.

For antenna correlation equal to 0.9, the application of the reconfigurable scheme achieves a 12.34% improvement in the system throughput. The number of satisfied Web users increases from 3541 to 3969, equivalent to 12.03% improvement, whereas the number of satisfied FTP users is increased from 327 to 406, equivalent to 24.15% improvement. The number of satisfied system users is increased from 3868 to 4375, which represents an improvement of 13.1%. Finally it is worth mentioning that the reconfigurable algorithm, applied when the antenna correlation is high, slightly outperforms the conventional non-reconfigurable algorithm when the antenna correlation is ideal (equal to 0).

It should be further emphasized that a tight threshold has been selected to determine user satisfaction. In a realistic network, even when the user throughput is less than 95% of the service rate, the quality of service may still be sufficient. In order to obtain a better insight into the network's performance, it is interesting to investigate the distribution of the user throughput expressed as a percentage of the service rate. This information is depicted in Figure 9 for Web browsing users and in Figure 10 for FTP users, comparing reconfigurable and non-reconfigurable cases for antenna correlations equal to 0, 0.6, and 0.9. For Web browsing, 80% on the horizontal axis corresponds to a user throughput of 51.2 kbps, while for FTP, 80% corresponds to a user throughput of 307.2 kbps. It can be therefore observed that the majority of the network users are served with sufficient data rates for all the simulated test cases. Moreover, the impact of the increase in antenna correlation is quantified by the decrease in the number of users that are served with a throughput larger than 80% of the service rate. This performance degradation is rectified efficiently by applying the reconfigurable technique proposed in this paper.

7. CONCLUSIONS

In this paper, the system-level performance of an HSDPA multiple-antenna network, which employs space-time block coding schemes and supports reconfigurability to antenna correlation, was evaluated.

Reconfigurability was achieved at the link level by employing a linear precoder, which exploits the knowledge of long-term properties of the channel state information at the transmitter.

A link-to-system interface was applied, based on the instantaneous values of the channel capacity, in order to achieve a one-to-one mapping between a specific channel realization over a frame duration and the probability of frame error.

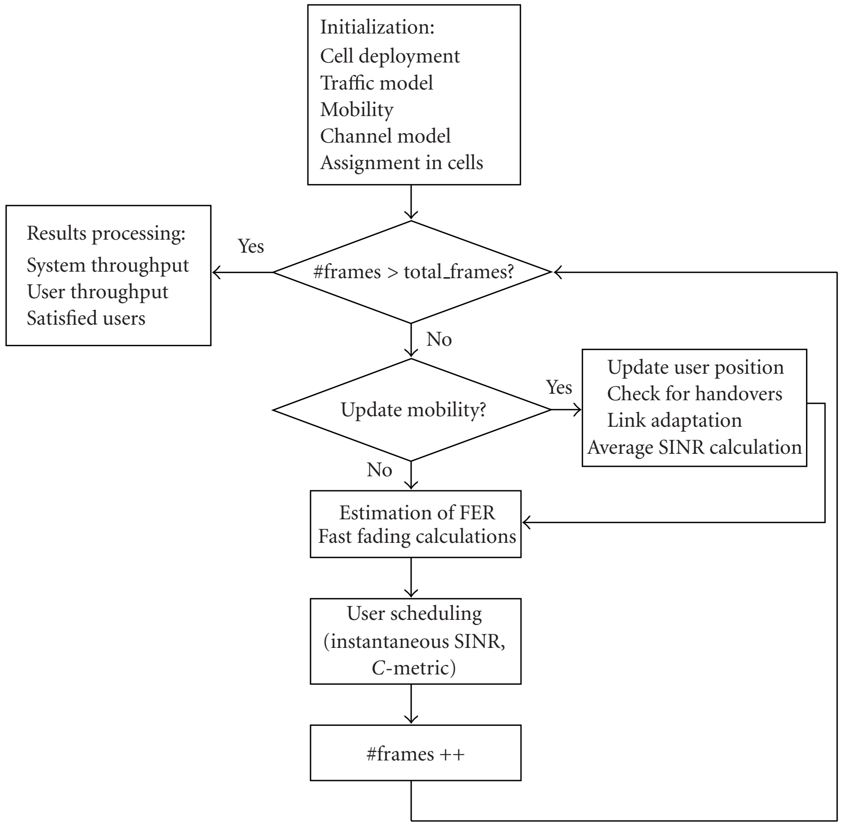

Figure 8: System-level simulation procedure flow chart.

Table 3: HSDPA system-level simulation results for 9 Mbps/sector traffic load.

Test cases	COR	Web users	FTP users	Satisfied Web users	Satisfied FTP users	Average system throughput (Mbps)	Satisfied Web users (%)	Satisfied FTP users (%)	Satisfied system users (%)
SISO	—	4818	528	2248	158	5.05	46.6	29.9	45.0
NRC	0	4818	528	3902	402	7.55	80.9	79.1	80.5
NRC	0.6	4818	528	3756	372	7.31	77.9	73.2	77.2
NRC	0.9	4818	528	3541	327	6.89	73.5	64.3	72.3
RC	0.6	4818	528	3885	392	7.51	80.6	77.1	80.0
RC	0.9	4818	528	3969	406	7.74	82.4	79.9	81.8

A system-level simulation methodology has been implemented taking into account fast fading and packet scheduling. The system-level performance was measured in terms of average system throughput and number of satisfied users. Web browsing and FTP services were considered in the simulations. It should be emphasized that in the simulation methodology presented herein, simplified assumptions on system-level functionalities were intentionally selected, as the objective was to investigate the system-level enhancements achieved by introducing reconfigurability in a space-time block coded system. Future studies could consider additional features of HSDPA, such as fast link adaptation and hybrid-automatic repeat request (H-ARQ).

System-level simulations were carried out for ideal, intermediate, and high antenna correlation conditions with nonreconfigurable and reconfigurable techniques. The degradation of the system performance was demonstrated for increasing antenna correlation. The application of the proposed reconfigurable technique was shown to efficiently compensate for the performance degradation for any value of the antenna correlation.

For intermediate antenna correlation values, the reconfigurable scheme was shown to achieve enhancements (over the conventional non-reconfigurable approach) of up to 3% in average system throughput and up to 5.5% in the number of satisfied users, whereas for high values of antenna correlation, the achieved improvements were 12% and 24%, respectively.

The system-level performance evaluation has proved that the application of the proposed reconfigurable technique

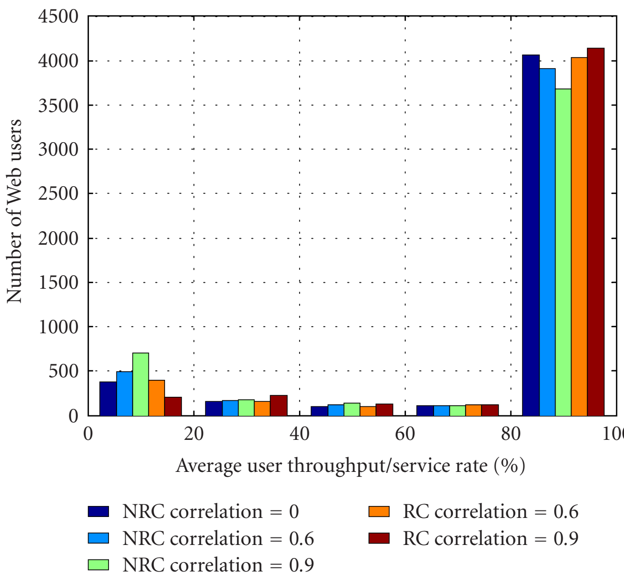

FIGURE 9: Distribution of the Web users average throughput expressed as a percentage of the service rate for reconfigurable (RC) and non-reconfigurable (NRC) Alamouti 2×2.

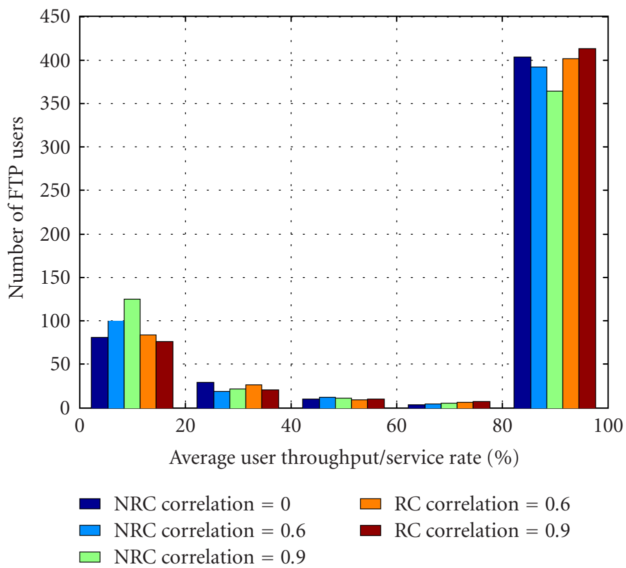

FIGURE 10: Distribution of the FTP users average throughput expressed as a percentage of the service rate for reconfigurable (RC) and non-reconfigurable (NRC) Alamouti 2×2.

is extremely valuable for heavily loaded HSDPA networks where high antenna correlation values are present.

ACKNOWLEDGMENTS

The work presented in this paper was performed within the framework of the IST FITNESS project (http://www.telecom.ece.ntua.gr/fitness). The authors would like to thank the anonymous reviewers for their comments and suggestions that considerably improved the presentation in this paper.

REFERENCES

[1] J. Salz and J. H. Winters, "Effect of fading correlation on adaptive arrays in digital mobile radio," *IEEE Trans. Veh. Technol.*, vol. 43, no. 4, pp. 1049–1057, 1994.

[2] D.-S. Shiu, G. J. Foschini, M. J. Gans, and J. M. Kahn, "Fading correlation and its effect on the capacity of multielement antenna systems," *IEEE Trans. Commun.*, vol. 48, no. 3, pp. 502–513, 2000.

[3] H. Bolcskei and A. J. Paulraj, "Performance of space-time codes in the presence of spatial fading correlation," in *Proc. 34th Asilomar Conference on Signals, Systems and Computers (ASILOMAR '00)*, vol. 1, pp. 687–693, Pacific Grove, Calif, USA, October 2000.

[4] C. Brunner, J. Hammerschmidt, and J. Nosek, "Downlink eigenbeamforming in WCDMA," in *Proc. European Wireless (EW '00)*, Dresden, Germany, September 2000.

[5] H. Sampath and A. J. Paulraj, "Linear precoding for space-time coded systems with known fading correlations," *IEEE Commun. Lett.*, vol. 6, no. 6, pp. 239–241, 2002.

[6] S. M. Alamouti, "A simple transmit diversity technique for wireless communications," *IEEE J. Select. Areas Commun.*, vol. 16, no. 8, pp. 1451–1458, 1998.

[7] V. Tarokh, N. Seshadri, and A. R. Calderbank, "Space-time codes for high data rate wireless communication: performance criterion and code construction," *IEEE Trans. Inform. Theory*, vol. 44, no. 2, pp. 744–765, 1998.

[8] H. Jafarkhani, "A quasi-orthogonal space-time block code," *IEEE Trans. Commun.*, vol. 49, no. 1, pp. 1–4, 2001.

[9] A. Alexiou and M. Qaddi, "Re-configurable linear precoders to compensate for antenna correlation in orthogonal and quasi-orthogonal space-time block coded systems," in *Proc. IEEE 59th Vehicular Technology Conference (VTC '04)*, vol. 2, pp. 665–669, Milan, Italy, May 2004.

[10] IST FITNESS Project, "Performance Metrics, Critical Parameters and Simulation Platforms," Deliverable D2.1, March 2002, http://www.telecom.ece.ntua.gr/fitness.

[11] A. Alexiou and M. Qaddi, "Robust linear precoding to compensate for antenna correlation in orthogonal space-time block coded systems," in *Proc. 3rd IEEE Sensor Array and Multichannel Signal Processing Workshop (SAM '04)*, Barcelona, Spain, July 2004.

[12] E. Telatar, "Capacity of Multi-Antenna Gaussian Channels," Technical Memorandum, AT&T-Bell Laboratories, Murray Hill, NJ, USA, 1995.

[13] Lucent Technology, "Throughput simulations for MIMO and transmit diversity enhancements to HSDPA," 3GPP TSG RAN WG1, TSGR1#17(00)1388, 2000.

[14] IST-FITNESS D3.3.1, "MTMR Baseband Transceivers Needs for Intra-system and Inter-system (UMTS/WLAN) Reconfigurability," http://www.telecom.ece.ntua.gr/fitness.

[15] IST-FITNESS D4.1, "Definition of system simulation methodology for UMTS and HIPERLAN/2," http://www.telecom.ece.ntua.gr/fitness.

[16] 3GPP TR 25.848, "Physical layer aspects of UTRA High Speed Downlink Packet Access".

[17] H. Bolcskei, D. Gesbert, and A. J. Paulraj, "On the capacity of OFDM-based spatial multiplexing systems," *IEEE Trans. Commun.*, vol. 50, no. 2, pp. 225–234, 2002.

[18] 3GPP Contribution, Lucent, "System Simulations for MIMO enhancements to HSDPA," TSGR1#16(01)0304.

[19] S. Hämäläinen, H. Holma, and K. Sipilä, "Advanced WCDMA radio network simulator," in *Proc. IEEE Symposium on Personal, Indoor and Mobile Radio Communications (PIMRC '99)*, pp. 951–955, Osaka, Japan, September 1999.

[20] J. Ramiro-Moreno, K. I. Pedersen, and P. E. Mogensen, "Network performance of transmit and receive antenna diversity in HSDPA under different packet scheduling strategies," in *Proc. IEEE Vehicular Technology Conference (VTC '02)*, vol. 1, pp. 482–486, Vancouver, British Columbia, Canada, September 2002.

[21] K. I. Pedersen and P. E. Mogensen, "Performance of WCDMA HSPDA in a beamforming environment under code constraints," in *Proc. IEEE 58th Vehicular Technology Conference (VTC '03)*, vol. 2, pp. 995–999, Orlando, Fla, USA, October 2003.

Kostas Peppas was born in Athens in 1975. He obtained his Diploma in electrical and computer engineering from the Department of Electrical and Computer Engineering, NTUA, in 1997, and the Ph.D. degree in wireless communications from the same department in 2004. His current research interests include wireless and personal communication networks, system-level analysis and design, signal processing, and applied mathematics.

Angeliki Alexiou received the Diploma in electrical and computer engineering from the National Technical University of Athens in 1994 and the Ph.D. degree in electrical engineering from Imperial College of Science, Technology and Medicine, University of London, in 2000. Since January 1999 she has been a member of technical staff in the Wireless Research Department, Bell Laboratories, Lucent Technologies, Swindon, UK, where she is involved in the development of advanced signal processing techniques for wireless communications. Her current research interests include multiple-antenna communications, signal processing for future-generation wireless systems, spatio-temporal channel modelling, and reconfigurable wireless systems supporting adaptivity to varying network conditions. Dr. Alexiou is a corecipient of Bell Labs President's Gold Award in 2002 for contributions to Bell Labs Layered Space-Time (BLAST) project and the Central Bell Labs Teamwork Award in 2004 for role model teamwork and technical achievements in the IST FITNESS project. Dr. Alexiou is the Vice Chair of the Working Group on New Air Interfaces, Relay-Based Systems, and Smart Antennas of the Wireless World Research Forum. She is a Member of the IEEE, the IEE, and the Technical Chamber of Greece.

Fotis Lazarakis received the Diploma in physics in 1990 from the Aristotle University of Thessaloniki, Greece, and the Ph.D. degree in mobile communications in 1997 from the National University of Athens. From 1999 to 2002 he was with Telecommunications Laboratory, NTUA, and then with the Institute of Informatics and Telecommunications, National Center for Scientific Research "Demokritos," as a researcher. His research interests include 3G and 4G systems, WLANs, and smart antenna systems. Dr. Lazarakis has authored more than 20 journal and conference papers.

Tareq Al-Gizawi received his Ph.D. degree in 4G mobile communications in 2005 from the Department of Electrical and Computer Engineering, National Technical University of Athens (NTUA), Greece. His main research area is 4G mobile communication systems, specifically mechanisms and algorithms that enhance seamless interworking between heterogeneous networks in the 4G environment. He is currently the General Manager of the Business Telecommunication Solutions (BTS) Company. BTS develops WiFi solutions and innovative WLAN applications. Dr. Al-Gizawi has authored more than 13 journal and conference papers.

Dimitrios I. Axiotis received the Diploma in 1999 and the Ph.D. degree in 3G mobile communications in 2004, both from the Department of Electrical and Computer Engineering, National Technical University of Athens (NTUA), Greece. He is currently a Research Associate in Telecommunications Laboratory, NTUA, participating in FP5/FP6 research projects. His research interests involve HAPS-UMTS and interoperating HSDPA/WLAN networks enhanced with MIMO techniques. He has published over 20 papers and serves as a reviewer in international journals and conferences. Dr. Axiotis is a Member of IEEE and the Technical Chamber of Greece.